INTERNATIONAL JOURNAL OF PRECISION ENGINEERING AND MANUFACTURING-GREEN TECHNOLOGY Vol. 5, No. 2, pp. 247-254 APRIL 2018 / 247

REGULAR PAPER

DOI: 10.1007/s40684-018-0025-6
ISSN 2288-6206 (Print) / 2198-0810 (Online)

An Analysis of Pinned Edge Layer of Slot-Die Coated Film in Roll-to-Roll Green Manufacturing System

Janghoon Park[1], Sungyong Kim[2], and Changwoo Lee[2,#]

1 Department of Polymer Science and Engineering, University of Massachusetts Amherst, 120 Governors Drive, Amherst, Massachusetts, 01003, USA
2 School of Mechanical Engineering, Changwon National University, 20, Changwondaehak-ro, Uichang-gu, Changwon-si, Gyeongsangnam-do, 51140, Republic of Korea
Corresponding Author / E-mail: changwoo1220@iCloud.com, TEL: +82-55-213-3618
ORCID: 0000-0001-9862-2833

KEYWORDS: Roll-to-roll, Slot-die, Adhesive, Pinned edge, Computational fluid dynamics, Solar cells

Roll-to-roll slot-die manufacturing of soluble materials with a uniform layer is a critical step in realizing low-cost and eco-friendly printed electronics for solar cells and batteries. This study presents an analysis of the lateral thickness of a coated layer that consists of a fluid with a high viscosity produced by using a slot-die roll-to-roll system with specific attention focused on a pinned edge phenomenon exhibited in the coated layer. A solution viscosity of 832 mPa·s is used and includes relatively high capillary numbers in the experiment in the range of 0.47–3.47. The purpose of the study included analyzing various forces around the coating nozzle and determining the correlation between forces by using dimensionless numbers. Computational fluid dynamics analysis and experiments were performed to obtain various parameters in terms of these dimensionless numbers. The experimental results suggest that the pinned edge should be reduced below 10% by reducing the coating gap parameter that represents the gravity forces.

Manuscript received: April 21, 2017 / Revised: November 15, 2017 / Accepted: December 6, 2017

NOMENCLATURE

t = Time
ρ = Density
p = Pressure
μ = Viscosity
$\mathbf{v}$ = Fluid flow velocity vector field
$\mathbf{g}$ = Gravity vector field
m = Mass
$\mathbf{A}$ = Area of the inlet vector field
v_{in} = Velocity inputs
v_{out} = Velocity outputs
v_i = ith Sampled output velocity
M = Mean value of the data set
Σ = Standard deviation of the data set
x_i = ith thickness of the coated layer
U = Percentage of uniformity variation
F_i = Inertia forces
F_g = Surface tension forces
F_σ = Gravity forces
F_μ = Viscous forces
Ca = Capillary number
Re = Reynolds number
St = Stokes number
Fr = Froude number
V = Coating velocity
H = Coating gap
σ = Surface tension of the liquid
g = Acceleration of gravity

1. Introduction

The slot-die coating method is highlighted as a cost-effective, eco-friendly, and scalable process technology for thin film production and can be utilized to formulate functional layers in electronic devices such as solar cells, sensors, fuel cells, and batteries.[1-5] The primary advantage of the slot-die coating process corresponds to predicting layer thickness,[6] in which the thickness of a coated layer can be controlled by adjusting coating process conditions.

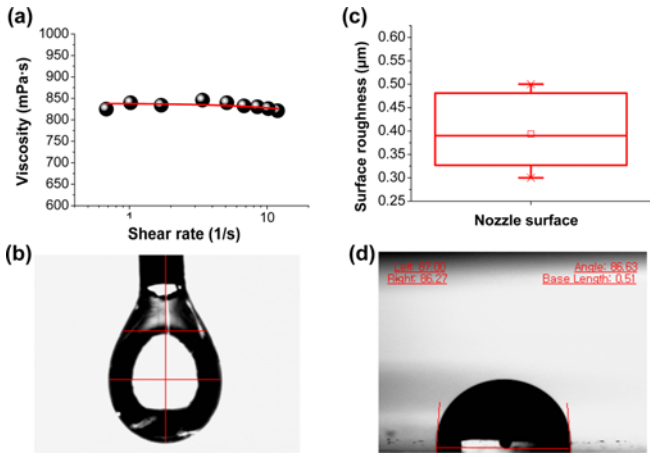

Fig. 1 Measurement of the properties of the materials: (a) the viscosity of the adhesive liquid based on changes in the shear rate, (b) the pendant drop method to measure the surface tension of the adhesive, (c) the surface roughness values of the surface inside the slot-die nozzle, and (d) the contact angle with respect to the nozzle surface with DI water

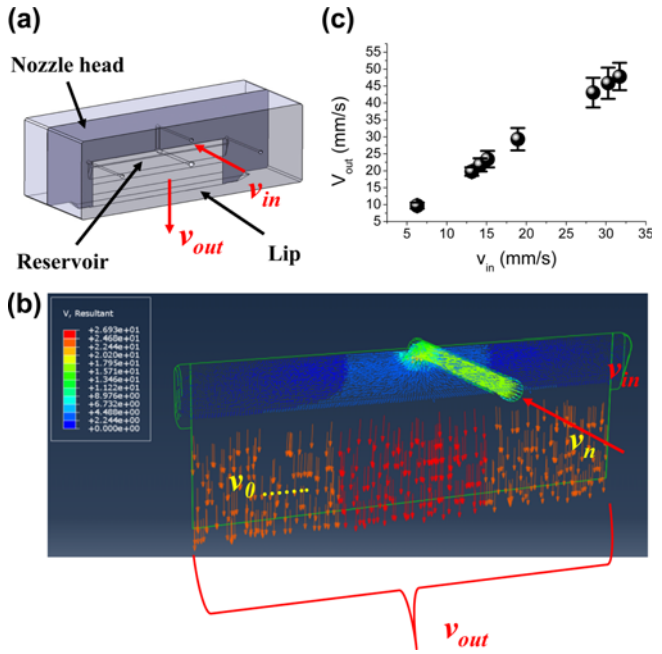

Fig. 2 (a) Three-dimensional modeling of the slot-die nozzle using actual dimensions, (b) the results of an Abaqus simulation showing the velocity profile near the outlet of the nozzle, and (c) the simulated output velocity profile at the exit of the nozzle outlet relative to the velocity at the nozzle inlet

In order to produce a thinner film or to develop more controllable film coating processes, it is necessary to consider various factors involved in the coating process. Higgins and Scriven derived a mathematical model for an achievable minimum wet thickness based on the operating limits of the capillary number.[7] The model showed that a coated thickness could be obtained by using a combination of the coating gap, viscosity, surface tension of the fluids, and coating velocity. Additionally, the governing equation provides the origin of the pressure difference between the upstream and downstream meniscus near the slot-die nozzle. In order to form a meniscus that is nearly cylindrical in shape, it is necessary to precisely control the pressure in the slot-die nozzle. Thus, a vacuum box was developed to provide constant pressure control in the presence of variations in the operating conditions.[8]

Several researchers investigated these coating phenomena by using various scientific and numerical approaches including computational fluid dynamics (CFD) modeling.[9] A coating window was developed based on the capillary, Reynolds, Stokes, and Froude dimensionless numbers and is related to the ratio between the coating thickness and coating gap.[6,10] The window was subsequently extended by considering two-dimensional Navier-Stokes equations for the free surface of a coating bead.[11] Ji et al. introduced a coating window based on a viscocapillary model with a commercial CFD-solver.[12] Akbarzadeh and Hrymak observed the coating flow inside a nozzle by using CFD techniques and then extended their simulations to include three-dimensional flows for particle motion.[13] Chang et al. directly observed coating flow by using a microscope to obtain visualized flow near the sides of a nozzle.[14]

Recently, slot-die coatings were applied using a roll-to-roll (R2R) system,[3,15] which is representative green manufacturing technology and based on a web substrate as opposed to a rigid substrate, and the characteristics produced by associated processes were analyzed from a statistical viewpoint.[16-19] In contrast to lab scale coating methods, the R2R coating process is specifically targeted at industries that continuously require large-area films that are wider than 150 mm and longer than 100 m.[20,21] Several researchers attempted to analyze the coating phenomena on a lab scale and focused on the microscopic region. However, with respect to the R2R process, it is important to also consider the thicknesses in both the lateral and longitudinal directions due to the wide coating area. A previous study[17] identified process conditions including the coating velocity and coating gap as significant factors that affect lateral thickness. Furthermore, the results indicated that pinned edges developed in a 150 mm wide coated layer and extant studies indicated that a wide coated layer in a 4 mm strip can result in pinned edges caused by a coffee-ring effect.[22] The pinned edge can degrade the multi-layered coating films of R2R processed organic photovoltaics and must be improved.[23]

In this study, the effects of process conditions as well as the effects of fluid flows inside a slot-die nozzle are investigated. Specifically, an understanding of the nozzle flows and the velocity of the flow inside the nozzle enables analysis of the correlation between various forces, such as viscous, surface tension, inertia, and gravity forces, around the slot-die nozzle based on dimensionless numbers.[10,24] This approach is similar to the one adopted by Bhanmidipati et al. from a perspective of air entrainment in the slot-die coating process.[25,26]

In the present study, R2R slot-die coating with a high-viscosity adhesive liquid was demonstrated. The selected adhesive materials are commonly used in the lamination film and protective tape industries.[27,28] The coated film was evaluated using a surface profiler to obtain thickness in the lateral direction. A CFD simulation was conducted using commercial software based on the measurement

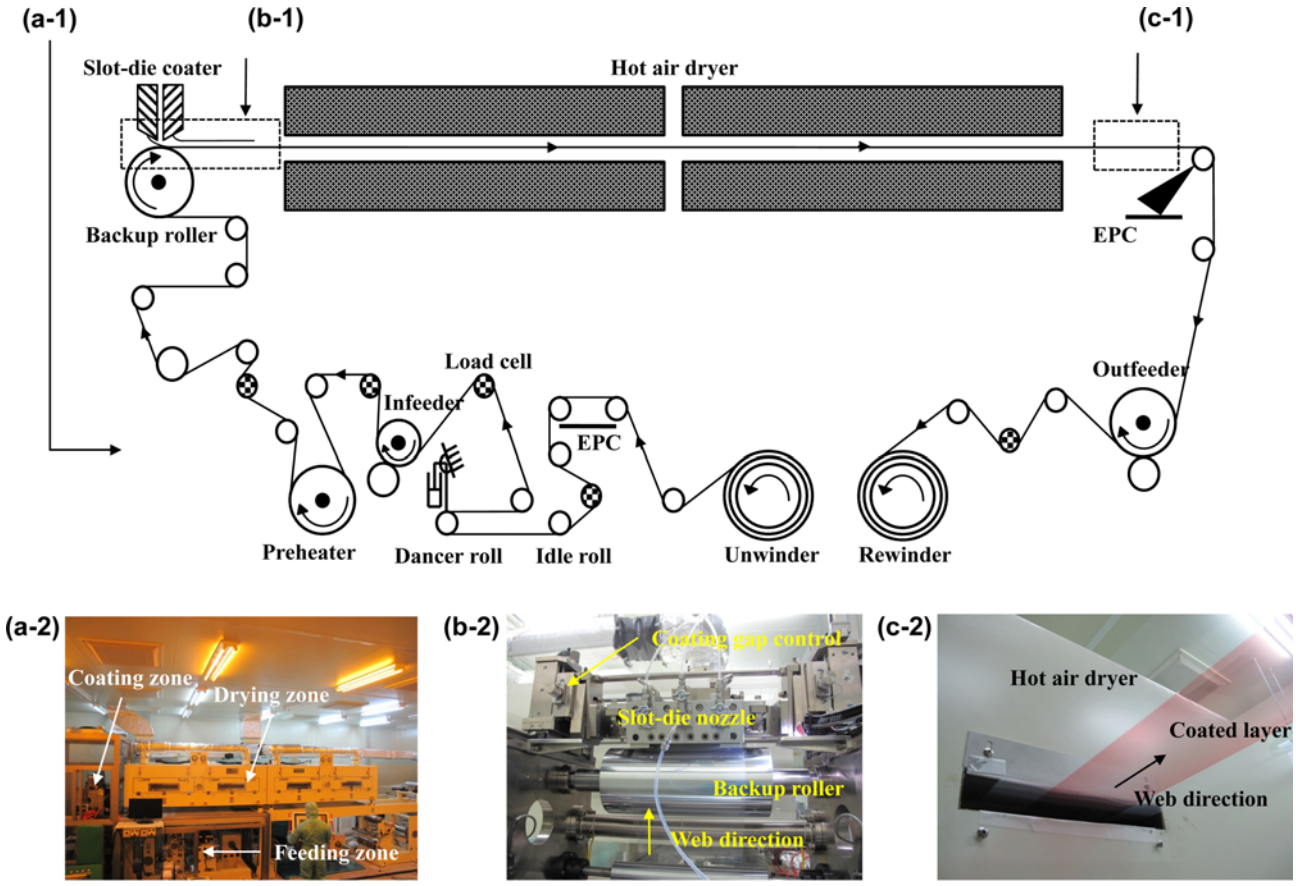

Fig. 3 (a) R2R system, (b) slot-die coating zone, and (c) coated product after drying

results to determine the properties of the liquid and the slot-die nozzle. In the simulation results, the output coating profile was evaluated in the lateral direction and compared with the measured thickness values. Based on the simulation results, the results of the analysis on the dimensionless numbers were discussed to explain the effects of the various forces around the nozzle that are correlated to the lateral coating profiles.

2. Materials Properties

The selected coating liquid corresponded to an adhesive material (SAIVINOL, PL-8540), which was mixed with ethyl acetate at a ratio of 40 wt%. The slot-die nozzle (Naraenanotech Co., Ltd, Korea) was fabricated from stainless steel and precisely processed in order to obtain a uniform surface. The properties of the fluid and slot-die nozzle were obtained by using the measurements depicted in Fig. 1 to perform a CFD simulation. The dynamic viscosity of the coating liquid was measured using a viscometer (GV-3003, Brookfield Co., Ltd) and corresponded to 832±7.7 mPa·s, as shown in Fig. 1(a). Based on this result, it was determined that the fluid possessed Newtonian characteristics. The surface tension of the liquid corresponded to 40 mN/m as shown in Fig. 1(b) when measured by using a contact angle meter (GSA, Surface Tech. Co., Ltd, Korea) with a pendant drop method. The viscosity of the coating solution was high such that the liquid was controlled by a syringe pump (Legato 100, KD Scientific, USA). The surface roughness of the slot-die nozzle as measured by using an interferometer (NV-2000, Nanosystems Co., Ltd, Korea) as shown in Fig. 1(c) corresponded to 391 nm (root mean square). The surface energy inside the slot-die nozzle was measured to be 28.46 mN/m by using a contact angle meter, as shown in Fig. 1(d). The density was calculated to be 0.96 g/cm^3 based on measurements of the weight and volume of the liquid. The kinetic eddy viscosity was calculated to be 0.001875 m^2/s by using the equation $\nu=\mu/\rho$ (ν: kinematic viscosity, μ: viscosity of fluid, ρ: fluid density).

3. Numerical Analysis

The flow of the coating fluid is governed by continuity and incompressible equations for a viscous fluid with a constant fluid viscosity as shown in Eqs. (1) and (2)[29,30] as follows:

$$\nabla \cdot v = 0 \tag{1}$$

$$\rho\left(\frac{\delta v}{\delta t} + v \cdot \nabla v\right) = -\nabla p + \mu \nabla^2 v + \rho g \tag{2}$$

The three-dimensional model of the slot-die nozzle is shown in Fig. 2(a) and is based on the actual dimensions of the fabricated slot-die. The boundary conditions for the simulation include the following. The pressure was set as zero based on an assumption by Harris, et al.[31] in which the pressure is uniformly distributed across the slot-die. The

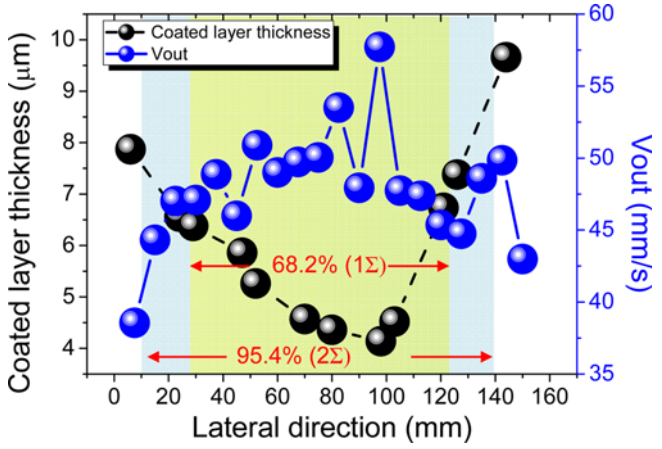

Fig. 4 Comparison between the measured coated layer thickness and the simulation results of the output velocity of the fluid near the nozzle lip. The colored regions indicate the 1σ-width and 2σ-width standard deviations

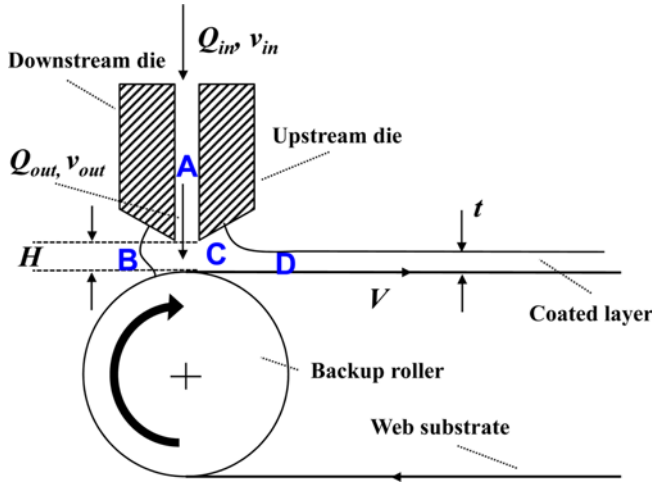

Fig. 5 Schematic diagram of the slot-die coating process and a depiction of the associated forces (A-D), where Q_{out}, Q_{in}, and t correspond to the flow rate at the outlet of the nozzle, the flow rate at the inlet of the nozzle, and the dried thickness of the coated layer, respectively

velocity condition is set for an incompressible flow as shown in Eq. (3) given below:

$$\dot{m} = \rho A \cdot v \tag{3}$$

There was no temperature change in the slot-die coating process, and thus the temperature condition was fixed at 25°C. The no-slip boundary condition is assumed on the inlet and inside of the slot-die nozzle surface as shown in Eq. (4) given below:

$$v = 0 \tag{4}$$

In Fig. 2(a), the nozzle diameter of the inlet corresponds to 6 mm, and the outlet area corresponds to 150 mm × 120 μm. The reservoir inside the nozzle plays a role in consolidating and stabilizing the fluids, and the nozzle design includes several special curves whose the details are the confidential property of the company that manufactured the slot-die.

The simulation is conducted using the Abaqus software (Dassault Systèmes, France). The simulation is conducted by using velocity inputs v_{in} of 6.3, 13.1, 14.2, 15.1, 18.9, 28.4, 30.3, and 31.7 mm/s. Fig. 2(b) shows the results of the CFD analysis with a v_{in} of 15.1 mm/s. The flows in the inlet exhibit a velocity of 13-15 mm/s. In the reservoir, the liquids are spread out near the sides, and the velocity at the edge is lower than the velocity at the center point. The output fluid velocity v_{out} increases significantly near the lip of the nozzle when it flows through an extremely narrow slot gap of 120 μm. The velocity increases to 27 mm/s at its highest point. In contrast, the velocity near the edge corresponds to 24.6 mm/s, which is lower than the velocity at the center point. As a result, it is assumed that the differences in v_{out} between the center and the edge affect the coating profile because when fluids strike a moving web (wall) that is perpendicular to the direction of the stream, the velocity differences can cause the fluid to flow sideways across the web.

Fig. 2(c) shows the profile of v_{out} based on the changes in v_{in}. The velocity v_{out} is measured at 20 points in the lateral direction, and the points are separated by a gap of 7.5 mm. The velocities at the 20 points are denoted from v_0 to v_n where v_n indicates the nth velocity profile. With respect to an evaluation of the output velocity profile, the representative value for v_{out} is defined based on Eq. (5) as follows:

$$v_{out} = \frac{\sum_{i=1}^{n} v_i}{n} \tag{5}$$

The graph also shows that the deviations in the output velocity profile are proportional to the changes in v_{in}. Thus, v_{out} can be used as a representative value while determining the correlation between the coating flows (the fluid velocity distribution) and the lateral thickness profile.

4. Experimental

An R2R slot-die coating experiment was performed. Fig. 3 shows the R2R slot-die coating system and the associated process. As shown in the figure, the R2R system consisted of a number of rollers and motors. A web substrate (SH-34, SKC Co., Ltd, Korea) was linked from the unwinder to the rewinder with a tension of 9.8 N. The tension was precisely controlled as the web passed through the edge position controller (EPC), dancer roll, infeeder, preheater, and backup roller as shown in Fig. 3(a).[32] The slot-die coater was installed on the backup roller with variable coating gaps of 100 μm, 150 μm, 200 μm, 300 μm, 350 μm, and 400 μm as shown in Fig. 3(b). The coating gap affects the coating thickness, and thus the gap setting module was designed with a high resolution of 5 μm. The coating velocity (web velocity) was selected to be 2 m/min, 6 m/min, or 10 m/min. The flow rate of the liquid was controlled by a mono pump (3NBL04F, Heishin Co., Ltd,

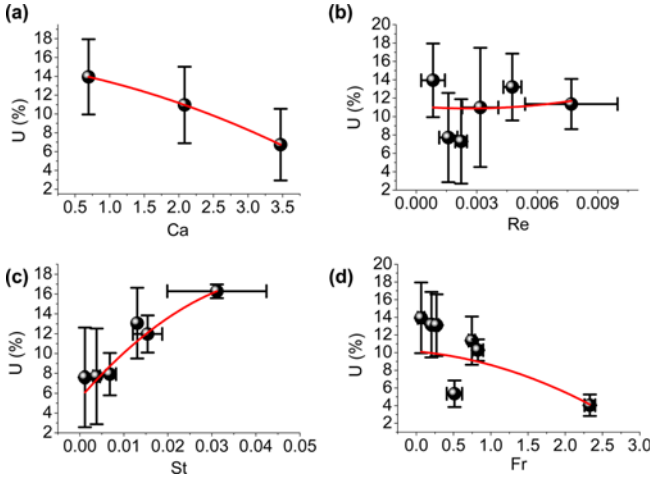

Fig. 6 Defined percentage of uniformity as a function of the various dimensionless numbers in the coating experiment: (a) *Ca*, (b) *Re*, (c) *St*, and (d) *Fr*

Japan) to be 10.7 mL/min, 22.3 mL/min, 24 mL/min, 25.6 mL/min, 32 mL/min, 48.1 mL/min, 51.3 mL/min, and 53.8 mL/min, which was matched to the simulated data shown in Fig. 2(c). The coated adhesive layer was uniformly dried in a hot air drying section. In order to clearly observe the coated layer, a red color pigment (ORIKO RED 236, Orient chemical Co., Ltd, Korea) was added to the coating liquid as shown in Fig. 3(c). The thickness of the coated layer was measured by using an interferometer, and the layer was physically removed and measured to determine the thickness in the lateral direction because the interferometer could measure a distance of 5 mm from the base substrate. The measurement procedures were the same as those detailed in a previous study.[17]

5. Results and Discussion

Both the thickness profile of the coated layers and the simulated v_{out} under the following conditions, namely a 6 m/min coating velocity, 350 μm coating gap, and 32.07 mm/min flow rate, exhibited pinned edges as shown in Fig. 4. The coated layer thickness included pinned edges with a large gap with a thickness of 5.5 μm from the bottom to the top. Additionally, the CFD simulation results from the Abaqus software showed an inversely proportional distribution profile for the output velocity. This result implies that there is a correlation between the coating flows and the lateral thickness of the layer.

Here we assumed that the coffee-ring effect and the Marangoni effect were negligible since we used a high-viscosity polymer material rather than a colloid-based solution.[33] It is not possible to determine thickness if an absolute difference is observed between the edge the effect of the average s and the center. Hence, the standard deviation was adopted in order to evaluate the thickness profile. The relative decrease in the pinned edges to the center is evaluated using Eqs. (6)–(8) as given below:

$$M = \frac{1}{n}\sum_{i=0}^{n-1} x_i \tag{6}$$

$$\Sigma = \sqrt{\frac{1}{n-1}\sum_{i=0}^{n-1}(x_i - M)^2} \tag{7}$$

$$U = \frac{2\Sigma - 1\Sigma}{M} \times 100 \tag{8}$$

2Σ is 95.4% within two standard deviations, and 1Σ is 68% within one standard deviation. Thus, U denotes the gradient of the outer thickness in a 30 mm band along each edge as shown in Fig. 4.

Chang et al.[10] and Romero et al.[34] mention four forces, namely the inertial forces (A: F_i), surface tension forces (B: F_σ), gravity forces (C: F_g), and viscous forces (D: F_μ), which are present around the slot-die nozzle and web substrate as shown in Fig. 5. The forces can be expressed as dimensionless numbers,[25] which correspond to the ratios between two forces, such as the capillary number (*Ca*), Reynolds number (*Re*), Stokes number (*St*), and Froude number (*Fr*), as defined in Eqs. (9)-(12) given below:

$$Ca = \frac{F_\mu}{F_\sigma} = \frac{\frac{\mu V}{H}}{\frac{\sigma}{H}} = \frac{\mu V}{\sigma} \tag{9}$$

$$Re = \frac{F_i}{F_\mu} = \frac{\rho v_{out}^2}{\frac{\mu V}{H}} = \frac{\rho v_{out}^2 H}{\mu V} \tag{10}$$

$$St = \frac{F_g}{F_\mu} = \frac{\rho g H}{\frac{\mu V}{H}} = \frac{\rho g H^2}{\mu V} \tag{11}$$

$$Fr = \frac{F_i}{F_g} = \frac{\rho v_{out}^2}{\rho g H} = \frac{v_{out}^2}{gH} \tag{12}$$

As shown in Fig. 6, four of the dimensionless numbers were evaluated to obtain the trend in terms of the percentage of uniformity variation, U. The values for *Ca* demonstrated a decreasing tendency in U as shown in Fig. 6(a). The *Ca* range corresponded to 0.47-3.47, and this is termed as the convergence region of wet thickness.[35] However, the pinned edge can be minimized with respect to the increase in *Ca*. Evidently, U improved with increases in *Ca* due to the increase in F_μ when compared with that of F_σ. There are three coating regions in the coating of Newtonian solutions.[6] In first region, the film thickness increases with Ca. The viscocapillary model proposed by Ruschak and Scriven explains the operating limits.[7,36] Theoretically, the film thickness in first region can be Ca to the power of 2/3. When Ca is further increased, there may be a second region where the wet thickness becomes independent of Ca. When Ca is even higher, the film thickness decrease phenomenon occurs. In this case, Re is more than 20 where the influence of the inertia force is increased.[10] In this experiment, Re is less than 1, suggesting that the process conditions are in the viscous region with the high-viscosity solutions. Conversely, the values for *Re* did not indicate a clear tendency with respect to U as shown in Fig. 6(b). Chang et al.[10] reported that the wet thickness is independent of *Re*, and thus U did not show a clear tendency in the experiment. Specifically, Re and coating thickness do not show a unique relationship in coatings of solutions with high viscosity or with moderate viscosity. In this study, the effect of viscous forces is large due to the use of high viscosity solution, but the influence of inertia

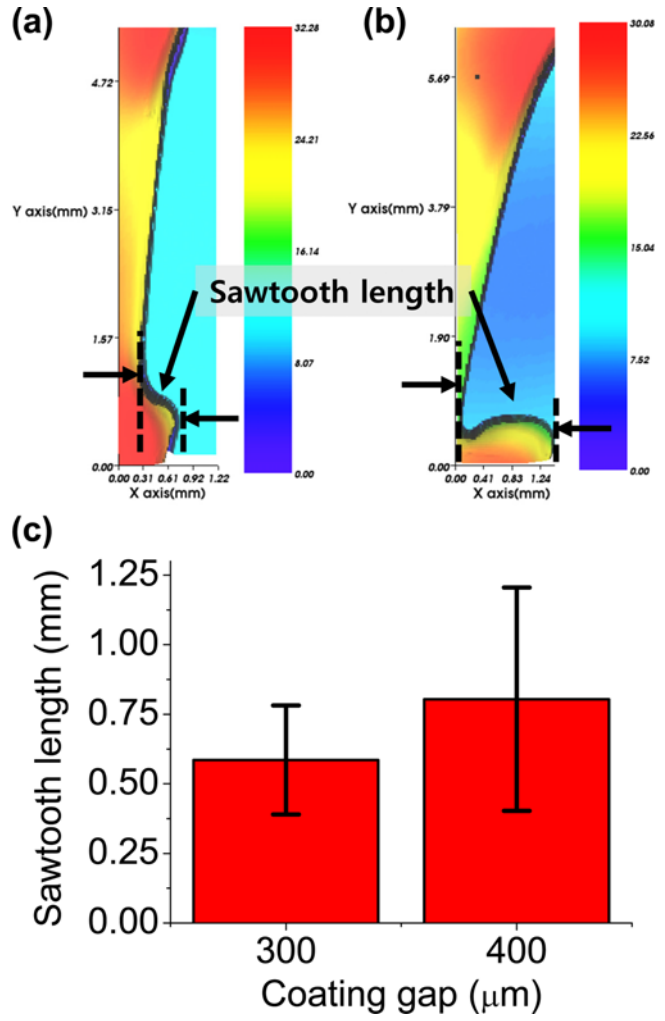

Fig. 7 Impact of the coating gap corresponding to (a) 300 μm and (b) 400 μm on the sawtooth length and (c) summarized results

forces is relatively small. In addition, the region of Re belongs to the first or the second region where the thickness is slightly increased or maintained.[6]

The increase in U led to an increase in St and a decrease in Fr as shown in Figs. 6(c) and (d). The fore-mentioned results clearly indicated that the Fg (i.e., gravity and the coating gap effect) is superior to $F\mu$ and Fi as demonstrated by the relationship between the numerator and denominator in Eqs. (11) and (12). The viscosity, gravity, and density corresponded to fixed values in the experiment, and the coating gap, H, output velocity, v_{out} and coating velocity, V corresponded to independent values. A high value of U indicated the presence of instabilities in the edge thicknesses. Based on the St and Fr numbers, the value of U ranged from 4% to 16%. Thus, relative differences in H, v_{out}, and V affect the value of U.

Extant research indicates that the effect of H is significantly related to the air entrainment in the coated layer.[25] An increase in H increased the air entrainment because of the increase in meniscus instability. The entrainment phenomenon is closely related to the dynamic contact angle. The dynamic contact angle changes with the coating gap and coating speed. Thus, the meniscus can be stabilized by reducing surface tension forces or increasing viscous forces. Previous studies have shown that the contact angle between die and downstream meniscus should be as small as 10°.[6] The value of F_σ is inversely proportional to the value of H, and thus the saw tooth can be more sensitive, which corresponds to a side effect of air entrainment. Fig. 7 shows the difference in sawtooth length with respect to the effect of H. The sawtooth was not present with respect to H values corresponding to 100 μm, 150 μm, and 200 μm. However, the conditions with a H value of 300 μm indicated a sawtooth corresponding to 0.384 mm as shown in Fig. 7(a), and a H value of 400 μm indicated a sawtooth corresponding to 1.088 mm as shown in Fig. 7(b). The coating edges of the H values indicated the generation of a sawtooth at 0.585 ± 0.2 mm and 0.804 ± 0.4 mm at 300 μm and 400 μm, respectively, of H [as shown in Fig. 7(c)]. Thus, the H is identified as a critical factor due to air entrainment for the uniformity of the edge thickness. Defect generation mechanism is still unclear. Defects are caused by limits of vacuum pressure, flow, dynamic wetting failure, and coating speed. Experimental studies have been conducted on this and additional information has been summarized in the previous study.[6]

In order to minimize U, it is necessary to reduce the coating gap and increase the coating velocity, which subsequently increases the F_μ ($\mu V/H$).[14] It is proven that an increase in F_μ minimizes the U as shown in Figs. 6(a) and (c). The inertia force, F_i, is known to exert a significant impact on the layer thickness in cases with high Ca values.[4] In this study, the F_i is closely related to the output velocity (v_{out}). Although it is clear that the v_{out} is correlated with U as indicated by Eq. (12), it is difficult to conclude the same based on the experimental results. As shown in Fig. 6(d), it is more reasonable to conclude that the tendency of U to decrease is due to the effect of the H and not to the v_{out}. Specifically, the effect of H is superior to the effect of v_{out} that introduces a clear decrease in U as the Fr decreases.

6. Conclusion

In this study, an R2R slot-die coated adhesive layer with a high viscosity corresponding to 832 mPa·s was evaluated from the viewpoint of lateral thickness. Dimensionless numbers, namely Ca, Re, St, and Fr, were examined to determine their correlation with lateral thickness. The forces around the slot-die nozzle consisted of inertia, surface tension, viscosity, and gravity forces. Specifically, it was difficult to measure the inertia forces at the outlet of the slot-die nozzle, and the velocity in the fore-mentioned region was assumed as a significant factor that affects the lateral thickness. Thus, CFD methodology was adopted to obtain the coating velocity profile near the nozzle. Based on the measured data, a CFD analysis was conducted using Abaqus software. The simulation results were compared with the results of an experiment that was performed by using a R2R slot-die coating system with adhesive materials. The novelty of the present study includes obtaining a phenomenon of pinned edges through a dimensionless analysis. A uniformity evaluation for the pinned edge was suggested based on 1-σ and 2-σ statistical methodologies. The results indicated that it was necessary to minimize the coating gap as the gravity force effect to enhance the viscous forces with respect to the St and Fr numbers. In cases in which the St was high, the pinned edge was increasingly pronounced while the Fr case showed an opposite tendency

due to air entrainment (unstable meniscus) in the high coating gap. Additionally, the findings indicated that the coating velocity with the viscous forces is the proven that can be minimized with respect to the pinned edges. In conclusion, the proposed dimensionless-number-based coating observation method can be useful in improving and understanding the R2R slot-die coating process in large-scale production situations of polymer solar cells, lightings, and printed batteries.

ACKNOWLEDGEMENT

This research was supported by National Research Foundation of Korea (NRF-2017R1A1A1A05001027)

REFERENCES

1. Park, J., Shin, K., and Lee, C., "Roll-to-Roll Coating Technology and its Applications: A Review," Int. J. Precis. Eng. Manuf., Vol. 17, No. 4, pp. 537-550, 2016.
2. Li, T. -C. and Chang, R. -C., "Improving the Performance of ITO Thin Films by Coating PEDOT: PSS," Int. J. Precis. Eng. Manuf.-Green Tech., Vol. 1, No. 4, pp. 329-334, 2014.
3. Roh, H. D., Lee, H., and Park, Y. -B., "Structural Health Monitoring of Carbon-Material-Reinforced Polymers Using Electrical Resistance Measurement," Int. J. Precis. Eng. Manuf.-Green Tech., Vol. 3, No. 3, pp. 311-321, 2016.
4. Lee, H., Jeong, J., Park, Y. -i., and Cha, S. W., "Energy Management Strategy of Hybrid Electric Vehicle Using Battery State of Charge Trajectory Information," Int. J. Precis. Eng. Manuf.-Green Tech., Vol. 4, No. 1, pp. 79-86, 2017.
5. Yim, C., Greco, K., Sandwell, A., and Park, S. S., "Eco-Friendly and Rapid Fabrication Method for Producing Polyethylene Terephthalate (PET) Mask Using Intensive Pulsed Light," Int. J. Precis. Eng. Manuf.-Green Tech., Vol. 4, No. 2, pp. 155-159, 2017.
6. Ding, X., Liu, J., and Harris, T. A., "A Review of the Operating Limits in Slot Die Coating Processes," AIChE Journal, Vol. 62, No. 7, pp. 2508-2524, 2016.
7. Higgins, B. and Scriven, L., "Capillary Pressure and Viscous Pressure Drop Set Bounds on Coating Bead Operability," Chemical Engineering Science, Vol. 35, No. 3, pp. 673-682, 1980.
8. Bassa, A. "Vacuum Box with Variable Stage Volume to Improve Coating Uniformity," US Patent, 4545321, 1985.
9. Cheema, T. A., Kim, K. W., Kwak, M. K., Lee, C. Y., Kim, G. M., et al., "Numerical Investigation on Composite Porous Layers in Electroosmotic Flow," Int. J. Precis. Eng. Manuf.-Green Tech. Vol. 1, No. 3, pp. 207-213, 2014.
10. Chang, H. M., Chang, Y. R., Lin, C. F., and Liu, T. J., "Comparison of Vertical and Horizontal Slot Die Coatings," Polymer Engineering and Science, Vol. 47, No. 11, pp. 1927-1936, 2007.
11. Carvalho, M. S. and Kheshgi, H. S., "Low-Flow Limit in Slot Coating: Theory and Experiments," AIChE Journal, Vol. 46, No. 10, pp. 1907-1917, 2000.
12. Ji, H. S., Ahn, W.-G., Kwon, I., Nam, J., and Jung, H. W., "Operability Coating Window of Dual-Layer Slot Coating Process Using Viscocapillary Model," Chemical Engineering Science, Vol. 143, pp. 122-129, 2016.
13. Akbarzadeh, V. and Hrymak, A., "Coupled Fluid-Particle Modeling of a Slot Die Coating System," AIChE Journal, Vol. 62, No. 6, pp. 1933-1939, 2016.
14. Chang, Y. -R., Chang, H. -M., Lin, C. -F., Liu, T. -J., and Wu, P. -Y., "Three Minimum Wet Thickness Regions of Slot Die Coating," Journal of Colloid and Interface Science, Vol. 308, No. 1, pp. 222-230, 2007.
15. Lee, J. -W. and Yoo, Y. -T., "A Comparative Study On Dimensional Stability of PET and BOPP Substrates for Fabrication of Flexible Electric/Electronic Devices Through Roll-to-Roll Printing," Journal of Industrial and Engineering Chemistry, Vol. 18, No. 5, pp. 1647-1653, 2012.
16. Park, J., Shin, K., and Lee, C., "Optimized Design for Anti-Reflection Coating Process in Roll-to-Roll Slot-Die Coating System," Robotics and Computer-Integrated Manufacturing, Vol. 30, No. 5, pp. 432-441, 2014.
17. Park, J., Shin, K., and Lee, C., "Improvement of Cross-Machine Directional Thickness Deviation for Uniform Pressure-Sensitive Adhesive Layer in Roll-to-Roll Slot-Die Coating Process," Int. J. Precis. Eng. Manuf., Vol. 16, No. 5, pp. 937-943, 2015.
18. Kang, H., Park, J., and Shin, K., "Statistical Analysis for The Manufacturing of Multi-Strip Patterns by Roll-to-Roll Single Slot-Die Systems," Robotics and Computer-Integrated Manufacturing, Vol. 30, No. 4, pp. 363-368, 2014.
19. Kang, H. and Lee, C., "Effect of Tension on Conductivity of Gravure Printed Ag Layer in Roll-to-Roll Process," Int. J. Precis. Eng. Manuf., Vol. 16, No. 1, pp. 99-104, 2015.
20. Shin, K., Park, J., and Lee, C., "A 250-Mm-Width, Flexible, and Continuous Roll-to-Roll Slot-Die Coated Carbon Nanotube/Silver Nanowire Film Fabrication and a Study on the Effect of Anti-Reflective Overcoat," Thin Solid Films, Vol. 598, pp. 95-102, 2016.
21. Lee, J. and Lee, C., "An Advanced Model for the Numerical Analysis of the Radial Stress in Center-Wound Rolls," International Journal of Mechanical Sciences, Vol. 105, pp. 360-368, 2016.
22. Etxebarria, I., Tait, J., Gehlhaar, R., Pacios, R., and Cheyns, D., "Surface Treatment Patterning of Organic Photovoltaic Films for Low-Cost Modules," Organic Electronics, Vol. 14, No. 1, pp. 430-435, 2013.
23. Krebs, F. C., "Polymer Solar Cell Modules Prepared Using Roll-to-Roll Methods: Knife-Over-Edge Coating, Slot-Die Coating and Screen Printing," Solar Energy Materials and Solar Cells, Vol. 93, No. 4, pp. 465-475, 2009.

24. Lin, C. F., Wong, H. D. S., Liu, T. J., and Wu, P. Y., "Operating Windows of Slot Die Coating: Comparison of Theoretical Predictions with Experimental Observations," Advances in Polymer Technology, Vol. 29, No. 1, pp. 31-44, 2010.

25. Bhamidipati, K., Didari, S., and Harris, T. A., "Experimental Study on Air Entrainment in Slot Die Coating of High-Viscosity, Shear-Thinning Fluids," Chemical Engineering Science, Vol. 80, pp. 195-204, 2012.

26. Bhamidipati, K. L., Didari, S., Bedell, P., and Harris, T. A., "Wetting Phenomena During Processing of High-Viscosity Shear-Thinning Fluid," Journal of Non-Newtonian Fluid Mechanics, Vol. 166, No. 12, pp. 723-733, 2011.

27. Park, G. H,, Kim, K. T., Ahn, Y. T., Lee, H. -I., and Jeong, H. M., "The Effects of Graphene on the Properties of Acrylic Pressure-Sensitive Adhesive," Journal of Industrial and Engineering Chemistry, Vol. 20, No. 6, pp. 4108-4111, 2014.

28. Fu, H., Yan, C., Zhou, W,. and Huang, H., "Nano-SiO2/fluorinated Waterborne Polyurethane Nanocomposite Adhesive for Laminated Films," Journal of Industrial and Engineering Chemistry, Vol. 20, No. 4, pp. 1623-1632, 2014.

29. Pedlosky, J., "Geophysical Fluid Dynamics," Springer Science and Business Media, 2013.

30. Batchelor, G. K., "An Introduction to Fluid Dynamics," Cambridge University Press, 1970.

31. Harris, T. A., Walczyk, D. F., and Weber, M. M., "Manufacturing of High-Temperature Polymer Electrolyte Membranes—Part I: System Design and Modeling," Journal of Fuel Cell Science and Technology, Vol. 7, No. 1, 011007, 2010.

32. Lee, J., Shin, K., and Lee, C., "Analysis of Dynamic Thermal Characteristic of Register of Roll-to-Roll Multi-Layer Printing Systems," Robotics and Computer-Integrated Manufacturing, Vol. 35, pp. 77-83, 2015.

33. Cui, L., Zhang, J., Zhang, X., Huang, L., Wang, Z., et al., "Suppression of the Coffee Ring Effect by Hydrosoluble Polymer Additives," ACS Applied Materials & interfaces, Vol. 4, No. 5, pp. 2775-2780, 2012.

34. Romero, O., Scriven, L., and Carvalho, M., "Slot Coating of Mildly Viscoelastic Liquids," Journal of Non-Newtonian Fluid Mechanics, Vol. 138, No. 2, pp. 63-75, 2006.

35. Lee, K. Y., Liu, L. D., and Ta-Jo, L., "Minimum Wet Thickness in Extrusion Slot Coating," Chemical Engineering Science, Vol. 47, No. 7, pp. 1703-1713, 1992.

36. Ruschak, K. J., "Limiting Flow in A Pre-Metered Coating Device," Chemical Engineering Science, Vol. 31, No. 11, pp. 1057-1060, 1976.